Published in final edited form as:

Nature. 2009 October 22; 461(7267): 1092–1097. doi:10.1038/nature08442.

SSB diffusion on single stranded DNA stimulates RecA filament formation

Rahul Roy[1,2,†], **Alexander G. Kozlov**[3], **Timothy M. Lohman**[3], and **Taekjip Ha**[1,2,4,*]

[1]Center for Biophysics and Computational Biology, University of Illinois, Urbana-Champaign, IL 61801, USA

[2]Department of Physics and Center for the Physics of Living Cells, University of Illinois, Urbana-Champaign, IL 61801, USA

[3]Department of Biochemistry and Molecular Biophysics, Washington University School of Medicine, St. Louis, MO 63110, USA

[4]Howard Hughes Medical Institute, Urbana, IL 61801, USA

Abstract

Single stranded (ss)DNA generated in the cell during DNA metabolism is stabilized and protected by binding of single stranded DNA binding (SSB) proteins. *E. coli* SSB, a representative homotetrameric SSB, binds to ssDNA by wrapping the DNA using its four subunits. However, such a tightly wrapped, high affinity protein-DNA complex still needs to be removed or repositioned quickly for unhindered action of other proteins. Here, we show, using single molecule two and three-color FRET, that tetrameric SSB can spontaneously migrate along ssDNA. Diffusional migration of SSB helps in the local displacement of SSB by an elongating RecA filament. SSB diffusion also melts short DNA hairpins transiently and stimulates RecA filament elongation on DNA with secondary structure. This first observation of diffusional movement of a protein on ssDNA introduces a new paradigm for how an SSB protein can be redistributed, while remaining tightly bound to ssDNA during recombination and repair processes.

SSB protein's primary activity in DNA metabolism is to bind preferentially to ssDNA with high affinity independent of sequence1. However, SSB proteins also play a central role by interacting with a large number of proteins, directing these proteins to sites of DNA replication, recombination or repair2. SSB proteins are often viewed as providing only inert protection for transiently formed ssDNA; however, there is increasing evidence that SSB-ssDNA complexes are highly dynamic which can be functionally important3-5. The *E. coli* SSB (*Eco*SSB) forms a stable homotetramer and can bind ssDNA in multiple modes with

[*]To whom correspondence should be addressed (tjha@illinois.edu)..

[†]Present Address: Department of Chemistry and Chemical Biology, Harvard University, Cambridge, MA 02138, USA

Author contributions. R.R., A.K., T.M.L. and T.H. designed the experiments, A.K. prepared the wild type SSB protein and the mutant SSB with fluorescent labels, R.R. performed the experiments and analyzed the data; R.R., T.M.L. and T.H. wrote the manuscript.

Supplementary Information is linked to the online version of the paper at www.nature.com/nature.

different properties6. In particular, under relatively high salt conditions (≥ 200 mM NaCl or ≥ 2 mM Mg^{2+} or polyamines), a low cooperativity complex forms in which ~65 nt of ssDNA wraps around the tetramer ($(SSB)_{65}$ mode), interacting with all four subunits such that the two ends of the ssDNA exit the protein in close proximity (referred to here as 'closed' wrapping)6,7.

Due to its transient role in replication, recombination and repair processes, SSB must be recycled (dissociate and reassociate with ssDNA) as well as repositioned within its ssDNA complexes. However, since *Eco*SSB binds with extremely high affinity to ssDNA making multiple binding interactions6, it remains unclear how SSB is displaced rapidly by other proteins, for example DNA polymerase or RecA, for subsequent DNA processing. Here, we demonstrate that an *Eco*SSB tetramer can migrate via a random walk along ssDNA thus providing a mechanism by which it can be repositioned along ssDNA while remaining tightly bound.

Diffusional migration of SSB on ssDNA

To investigate potential movements of SSB on ssDNA, we employed single molecule fluorescence resonance energy transfer (smFRET)8,9. FRET efficiencies *E* from individual immobilized partial duplex DNA with a 3' $(dT)_N$ tail ($64 \leq N \leq 131$) bound to SSB were acquired using total internal reflection fluorescence microscopy9. Surface immobilization and fluorescent labelling have no measurable effect on the dynamics of SSB binding mode transitions5. Owing to the closed wrapping in the $(SSB)_{65}$ binding mode favoured under our conditions (500 mM NaCl or 10 mM Mg^{2+})7, when SSB is bound to ssDNA of 65-70 nt with its two ends labelled with donor (Cy3) and acceptor (Cy5) fluorophores, singular high FRET distributions were observed5. However, when a $(dT)_{69}$ tail is further extended by an additional 12 nt of sequence complementary to the overhanging cohesive end of l-strand of λ phage DNA, individual SSB-ssDNA complexes display large FRET fluctuations in the millisecond time scale (Fig. 1a). These fluctuations were dramatically suppressed when the 12 nt extension is hybridized to a cohesive end of a λ DNA (Fig. 1b). To exclude binding and dissociation of additional SSB molecules as the cause of fluctuations, unbound SSB was removed by a buffer wash before measurements. DNA unwrapping/rewrapping dynamics, occurring in tens of microseconds in high salt3,4, is completely averaged out within our 10-30 ms time resolution5. We also ruled out local melting of the duplex portion as a source of fluctuations (Supplementary materials, SM1). Therefore, these fluctuations must arise from additional conformational states enabled by the 12 nt extension.

To test whether the FRET fluctuations are caused by transient excursions of SSB to the extension, we varied the length of the extension ($(dT)_N$, N= 0 - 18) while keeping the ssDNA between Cy3 and Cy5 at 69 or 70 nt. If an SSB tetramer binds randomly and remains fixed at the initial site of binding undergoing only transient interactions with ssDNA outside the binding site, each complex will generate a FRET distribution that is unique to the initial site of binding. However, all complexes for each construct displayed similar FRET time trajectories (Supplementary Fig. 1). Furthermore, if SSB migrates along the DNA, larger excursions away from the high FRET state are expected for longer extensions. Indeed, average FRET values decreased for longer extensions while the high FRET state was still

transiently visited (Supplementary Fig. 1). The FRET distribution and the time scale of fluctuations are relatively independent of the salt concentration (Supplementary Fig. 2), arguing against these FRET changes arising from binding mode transitions which display a strong salt dependence10-12. Hence, these fluctuations likely reflect SSB's diffusional migration on ssDNA with the different FRET values corresponding to different SSB locations.

To make unbiased assignments of FRET states, we employed a hidden Markov model (HMM) based statistical approach that determines the most likely time sequence of FRET states (Fig. 2a) 13,14. The result is further reduced to a transition density plot (TDP)13,14, that allows the number of distinct FRET states, their FRET values, and the transition rates to be estimated (Fig. 2b). We analyzed SSB migration on DNA molecules with several 3' dT tail lengths (0 to 12 nt extension beyond 65 nt binding site size) at 13 °C to slow down migration (Fig. 2a and b). Longer extensions gave multiple indistinguishable low FRET states in the TDP (Supplementary Fig. 3). For $(dT)_{69+8}$ (12 nt extension from the 65 nt binding site size with 69 nt separation between fluorophores), six distinct FRET states were resolved (Fig. 2b) with transitions occurring between nearest neighbours. We assigned the highest FRET value ($E \sim 0.8$) to the state with SSB closest to the ss-dsDNA junction and lower FRET values for positions away from the junction. The rates of transition, or the 'stepping rates', were independent of the beginning and ending state of transition (Supplementary Fig. 4) and ranged between 3.0 and 4.5 s^{-1} (Fig. 2c). Similar analysis yielded 5, 3 and 2 states for DNA with 8, 2 and 0 nt extensions, respectively (Supplementary Fig. 3). Therefore, every 2-4 nt of DNA extension provides an additional configuration, yielding an apparent step size of about 3 nt.

Because FRET fluctuations became too fast for HMM analysis above 13°C, we used autocorrelation analysis of FRET efficiency *E* for the temperature dependence studies (Fig. 2d). The averaged auto-correlation function plots of the SSB-$(dT)_{69+8}$ complexes were best fit by bi-exponential decays. The shorter lifetime was equal to the time resolution independent of temperature and is ascribed to photophysical or detection noise The longer lifetime, τ_{long}, displayed a monotonic temperature dependence and was attributed to SSB diffusion. The Arrhenius fit of $\ln(1/\tau_{long})$ vs. 1/T (Fig. 2e) gave an apparent activation energy of 81 ± 7 kJ/mol. Combined with the stepping rate of ~ 4 s^{-1} at 13 °C, we can then estimate a stepping rate of ~ 60 s^{-1} at 37 °C. Assuming a 3 nt step size, the diffusion coefficient of an SSB tetramer along ssDNA at 37 °C is estimated to be 270 $(nt)^2/s$.

As a further test of SSB migration on the ssDNA, we employed single molecule 3 color FRET9,15 using a donor-labelled SSB mutant (A122C labelled with ~1 Alexa555 per SSB tetramer) and two different acceptors, Cy5 and Cy5.5, attached to the two ends of a $(dT)_{130}$ (Fig. 3a). The large separation between the two acceptors eliminates any significant FRET between them. If a single SSB tetramer diffuses on the long ssDNA, high FRET events to either acceptor will be mutually exclusive. Indeed, we observed rapid and anti-correlated fluctuations of apparent FRET efficiencies to the two acceptors, $E_{app,5}$ and $E_{app,5.5}$, demonstrating that SSB truly diffuses on the DNA (Fig. 3a and b). To ensure single SSB molecules on DNA, 1 min incubation with sub-saturating concentrations of SSB (< 100 pM) was followed immediately with a buffer wash and only traces displaying single donor

photobleaching events were analyzed. At higher SSB concentration (10 nM), much slower FRET fluctuations were observed likely due to binding of additional SSB (Supplementary Figure 5).

To probe how far SSB can move on a long ssDNA, we placed Cy5 and Cy5.5 on the two ends of a $(dT)_{130}$ and Cy3 in the middle (named $(dT)_{65+65}$). This 3-color FRET scheme allows us to determine at which end the SSB was present by following the 'closed' wrapping of that DNA segment and high FRET to the corresponding acceptor (Fig. 3c). Both the dye pairs display transient high FRET states that are anti-correlated indicating that the same SSB molecule was capable of migrating to either end of the DNA (Fig. 3c and d). Therefore, SSB can move at least 65 nt via diffusion and is not constrained to its initial binding site.

SSB displacement by RecA filament

SSB modulates the interaction between the RecA protein and ssDNA in the SOS response and recombinational repair pathway2,16-19 and mutations in the *ssb* gene cause inefficient recombinational repair and homologous recombination1,20-22. A RecA filament can readily displace SSB from the DNA if assisted by RecFOR, χ-modified RecBCD or a preassembled nucleation cluster14,23-27. However, the mechanism of efficient SSB displacement by RecA was unclear given the tight binding of SSB to ssDNA.

Our estimated diffusion step size of SSB, ~ 3 nt, is the same as the binding site size of a RecA monomer which is the unit of filament extension14,28. We, therefore, hypothesized that a monomer-by-monomer addition of RecA to the DNA segment freed up by SSB diffusion might convert the random walk of SSB into unidirectional movement (Supplementary Movie 1). To test this idea, we devised a 3-color FRET assay using a DNA with a 96 nt 3' tail, $(dT)_{30+65}$, labelled at positions 0, 30 and 95 with Cy5.5, Cy3 and Cy5, respectively (Fig. 4). The apparent FRET efficiencies of DNA only are low for both acceptors (~0.1), and drops to zero upon RecA-ATPγS filament formation (Fig 4a and b). SSB addition after flushing out excess RecA and ATPγS removes the RecA-ATPγS filament from the ssDNA tail, but not from the duplex DNA14, and the ssDNA wraps around SSB,displaying higher FRET with a broad distribution that reflects SSB diffusion (Fig. 4c). The RecA-ATPγS filament remaining on the duplex serves as the nucleation cluster for filament elongation on the 3' ssDNA tail14 such that upon addition of RecA and ATP, the elongating filament rapidly replaces SSB on the ssDNA ($E_{app} = 0$) (Fig. 4e).

Fig. 4f shows the real time 3-color FRET trajectories of SSB displacement by an elongating RecA filament. Before elongation, the FRET values fluctuate rapidly due to SSB diffusion. Upon addition of RecA and ATP, $E_{app,5.5}$ drops first as a RecA-ATP filament initiates at the ss/dsDNA junction. As this filament grows further, $E_{app,5}$ attains a steady high value. Since the Cy3 and Cy5 are separated by 65 nt at the distal DNA end, we attribute this increase in $E_{app,5}$ to the repositioning of SSB to the distal end, pushed by the elongating RecA filament. Finally, complete filament elongation gives E_{app}~0, likely accompanied by SSB dissociation. Direct excitation of the acceptors afterwards confirmed that they were not photobleached.

We used exponential fits of average FRET curves to estimate the rates of three distinct events following the addition of RecA and ATP (Fig. 4g). (i) $E_{app,5.5}$ drops from 0.3 to 0 at a rate of $k_{1,SSB}$ = 0.24 ± 0.02 s^{-1}. We assign this to RecA filament initiation from the RecA-ATPγS nucleation site since once initiated, the decrease in $E_{app,5.5}$ is nearly instantaneous. (ii) $E_{app,5}$ increases from 0.3 to 0.75 at the rate of $k_{2,SSB}$ = 0.2 ± 0.01 s^{-1}. We assign this to RecA filament initiation and elongation by ~ 10 RecA monomers on 30 nt and SSB movement to the distal DNA end. The time intervals between the drop in the $E_{app,5.5}$ and the rise of $E_{app,5}$, place a lower limit of ~0.6 s^{-1} for the RecA elongation on a 30-mer of SSB-bound ssDNA (Supplementary Fig. 6). (iii) The decrease of $E_{app,5}$ (traces synchronized when the high $E_{app,5}$ state is obtained) that we assign to SSB dissociation occurs at a much lower rate of 0.07 ± 0.01 s^{-1}. The rates of filament initiation and elongation without SSB are comparable to those obtained with SSB (Fig. 4h and Supplementary materials, SM2). Furthermore, the rate of RecA elongation on bare ssDNA is about 20 s^{-1} per monomer at 1 μM RecA14 and is similar to the lower limit we determined here with SSB (~ 6 s^{-1} per monomer), suggesting that any hindrance to RecA elongation by SSB is minimal. Similar rates were observed on longer DNA where up to two SSB tetramers can bind (Supplementary Fig. 7).

Overall, the rate of SSB removal from the DNA end is ~ 10 fold slower than what is expected from filament elongation alone. This observation suggests that SSB diffusion is important for RecA filament elongation on SSB coated DNA. This is because before SSB hits the DNA end, its diffusion is isoenergetic and therefore is rapid, while its further diffusion at the 3' end is energetically costly. This model of rectifying the SSB diffusion by the directional growth of a RecA filament does not require any direct interaction of the two proteins29 and hence could provide a general mechanism for displacement of SSB by proteins moving directionally on the ssDNA.

SSB diffusion aids RecA on DNA hairpin

SSB inhibits RecA filament formation at low salt and high SSB concentrations23,29, but stimulates RecA filament formation in high salt29, likely by disrupting DNA secondary structures30,31. Tetrameric SSBs can in fact destabilize a DNA duplex possessing a single strand tail that is shorter than the SSB binding site size32 but no significant duplex disruption was observed for a tail length equal or greater than the binding site size (Fig. 1b and Supplementary materials, SM1). We therefore investigated whether SSB can disrupt a physiologically more relevant structure, that is, a hairpin flanked by two single stranded regions. The melting of a hairpin with a 7 bp stem and 3 nt loop, *hp*, (Fig. 5a) is monitored via FRET between Cy3 and Cy5 attached to the ends of the hairpin in two different constructs, $(dT)_{65+hp+3}$ and $(dT)_{6+hp+65}$. A single high FRET population for an intact hairpin is partially replaced by lower FRET populations with SSB, signifying different states of hairpin unzipping (Fig. 5b). Single molecule trajectories showed unzipping of the hairpin (Fig. 5c) with a majority displaying two-step unzipping with rate constants of ~ 1.1-1.5 s^{-1} (Fig. 5c and d; details in Supplementary materials, SM3). Hence, a single SSB tetramer transiently disrupts DNA secondary structures as stable as a 7 bp stem by repositioning itself on and off the hairpin segment.

Finally, we tested if such transient melting of a DNA hairpin by SSB promotes RecA filament formation on the hairpin. Starting from a pre-nucleated RecA-ATPγS complex, a RecA-ATP filament was formed on $(dT)_{6+hp+65}$ DNA (Fig. 5e) giving rise to a $E_{app} \sim 0$ population representing filament formation over the melted hairpin (Supplementary materials, SM4). Remarkably, filament formation over the hairpin occurred 40 fold faster when SSB is present, demonstrating that SSB stimulates filament elongation over ssDNA that can form stable secondary structures (Fig. 5f and Supplementary materials, SM4). Interestingly, for our second construct $(dT)_{65+hp+3}$, filament formation over the hairpin remained slow even with SSB (Fig. 5f). This dependence on hairpin position further indicates that transient hairpin disruption by SSB is necessary for efficient filament elongation for the following reason. RecA filament elongation towards the 3' end decreases the length of ssDNA available for SSB binding, forcing it to eventually dissociate. However, SSB dissociation occurs before the filament elongates to the hairpin region of $(dT)_{65+hp+3}$ such that SSB-induced hairpin melting is reversed prior to filament growth over the hairpin segment (Supplementary materials, SM4).

Based on these results, we propose that SSB diffusion along ssDNA in the low cooperative $(SSB)_{65}$ mode, where ssDNA is populated mostly with single or two tetramers33, stimulates RecA filament elongation by transiently removing DNA secondary structures ahead of the filament, and that filament elongation via RecA monomer addition in turn directionally biases SSB diffusion (Fig. 5g; Supplementary Movie 1). For long ssDNA bound by multiple SSB tetramers, directional migration of an SSB tetramer caused by RecA filament elongation may increase the local SSB concentration and promote transitions to other binding modes from which SSB dissociation may be much more rapid3,5. If so, the findings made here may also be relevant for the removal of multiple SSBs from longer ssDNA.

Mechanism and functions of SSB diffusion

How does SSB diffuse on ssDNA? One possibility is the previously suggested rolling mechanism ssDNA4,34. SSB rolling would occur via partial unwrapping of one end segment of ssDNA from an SSB tetramer followed by re-wrapping of the other end in its place (Supplementary Fig. 8 and Supplementary Movie 1), resulting in one dimensional random walk of SSB on ssDNA. Although our results are consistent with the rolling model, a definitive conclusion awaits further investigations.

Our work represents the first demonstration of any protein diffusing on ssDNA. By facilitating the redistribution of a tightly bound SSB tetramer along the ssDNA without full dissociation, SSB diffusion may be utilized in a variety of cellular processes, for example, stabilization of specific denaturation sites on superhelical DNA35,36 and facilitation of primase activity by positioning the SSB on G4 phage type priming systems37. The C-terminal region of *Eco* SSB interacts with a variety of DNA repair enzymes and facilitates localization of these enzymes in the vicinity of ssDNA38,39, raising the possibility that SSB acts as a mobile platform on the ssDNA for the repair and recombination machinery. The presence of homologous SSB proteins even in metazoans suggests that similar diffusion mechanism might operate over a wide range of species40.

Methods

Partial duplex DNA (18 bps dsDNA) with 3' $(dT)_N$ tails (N ranging from 64 to 131 nucleotides, nts) carrying one donor (Cy3) and up to two acceptors (Cy5 for two-color FRET, Cy5 and Cy5.5 for three-color FRET) were immobilized at the duplex end on polyethylene glycol coated surface using biotin-neutravidin and incubated with 100 pM - 1 nM SSB in imaging buffer for 1 min before flushing and single molecule data was acquired using wide-field total-internal-reflection (TIR) fluorescence microscopy9 with 8-100 ms time resolution. All single molecule measurements were performed at 23±1°C unless specified otherwise in imaging buffer (10mM Tris (pH 8.0), 500mM NaCl, 0.1mM Na_3EDTA, 0.1mg/ml BSA, oxygen scavenging system (0.5% w/v glucose, 1.5mM Trolox41 or 1% β-mercaptoethanol, 165U/ml glucose oxidase and 2170U/ml catalase). RecA-SSB experiments were conducted in 1 μM RecA (or 10nM SSB), 1 mM ATP (or 1 mM ATPγS) in 25 mM Tris acetate (pH 7.5), 50 mM Sodium acetate, 10 mM Magnesium acetate and 0.1 mg/ml BSA in combination with the oxygen scavenging system. Details of DNA sequences with modifications, annealing, reagents, experimental set-up and analysis indicated in the text are reported in Supplementary Methods.

Supplementary Material

Refer to Web version on PubMed Central for supplementary material.

Acknowledgements

We thank C. Joo, S. A. McKinney, I. Rasnik, S. Hohng and S. Myong for experimental help and discussion; C. Murphy, M. Nahas and K. Raghunathan for helpful discussion; T. Ho and A. Niedziela-Majka for help with DNA and protein preparation, respectively; and R. Porter for SSB expression plasmid. T.H. is an employee of the Howard Hughes Medical Institute. These studies were supported by grants from the National Institutes of Health and the National Science Foundation.

References

1. Meyer RR, Laine PS. The single-stranded DNA-binding protein of Escherichia coli. Microbiol Rev. 1990; 54:342–80. [PubMed: 2087220]
2. Shereda RD, Kozlov AG, Lohman TM, Cox MM, Keck JL. SSB as an organizer/mobilizer of genome maintenance complexes. CRC Reviews. 2008
3. Kozlov AG, Lohman TM. Kinetic mechanism of direct transfer of Escherichia coli SSB tetramers between single-stranded DNA molecules. Biochemistry. 2002; 41:11611–27. [PubMed: 12269804]
4. Kuznetsov SV, Kozlov AG, Lohman TM, Ansari A. Microsecond dynamics of protein-DNA interactions: direct observation of the wrapping/unwrapping kinetics of single-stranded DNA around the E. coli SSB tetramer. J Mol Biol. 2006; 359:55–65. [PubMed: 16677671]
5. Roy R, Kozlov AG, Lohman TM, Ha T. Dynamic structural rearrangements between DNA binding modes of E. coli SSB protein. J Mol Biol. 2007; 369:1244–57. [PubMed: 17490681]
6. Lohman TM, Ferrari ME. Escherichia coli single-stranded DNA-binding protein: multiple DNA-binding modes and cooperativities. Annu Rev Biochem. 1994; 63:527–70. [PubMed: 7979247]
7. Raghunathan S, Kozlov AG, Lohman TM, Waksman G. Structure of the DNA binding domain of E. coli SSB bound to ssDNA. Nat Struct Biol. 2000; 7:648–52. [PubMed: 10932248]
8. Ha T, et al. Probing the interaction between two single molecules: fluorescence resonance energy transfer between a single donor and a single acceptor. Proc Natl Acad Sci U S A. 1996; 93:6264–8. [PubMed: 8692803]

9. Roy R, Hohng S, Ha T. A practical guide to single-molecule FRET. Nat Methods. 2008; 5:507–16. [PubMed: 18511918]
10. Bujalowski W, Lohman TM. Escherichia coli single-strand binding protein forms multiple, distinct complexes with single-stranded DNA. Biochemistry. 1986; 25:7799–802. [PubMed: 3542037]
11. Lohman TM, Overman LB. Two binding modes in Escherichia coli single strand binding protein-single stranded DNA complexes. Modulation by NaCl concentration. J Biol Chem. 1985; 260:3594–603. [PubMed: 3882711]
12. Griffith JD, Harris LD, Register J 3rd. Visualization of SSB-ssDNA complexes active in the assembly of stable RecA-DNA filaments. Cold Spring Harb Symp Quant Biol. 1984; 49:553–9. [PubMed: 6397310]
13. McKinney SA, Joo C, Ha T. Analysis of single-molecule FRET trajectories using hidden Markov modeling. Biophys J. 2006; 91:1941–51. [PubMed: 16766620]
14. Joo C, et al. Real-time observation of RecA filament dynamics with single monomer resolution. Cell. 2006; 126:515–27. [PubMed: 16901785]
15. Hohng S, Joo C, Ha T. Single-molecule three-color FRET. Biophys J. 2004; 87:1328–37. [PubMed: 15298935]
16. Kowalczykowski SC. Initiation of genetic recombination and recombination-dependent replication. Trends in Biochemical Sciences. 2000; 25:156–165. [PubMed: 10754547]
17. Kowalczykowski SC, Dixon DA, Eggleston AK, Lauder SD, Rehrauer WM. Biochemistry of homologous recombination in Escherichia coli. Microbiol Rev. 1994; 58:401–65. [PubMed: 7968921]
18. Roca AI, Cox MM. RecA protein: structure, function, and role in recombinational DNA repair. Prog Nucleic Acid Res Mol Biol. 1997; 56:129–223. [PubMed: 9187054]
19. Kuzminov A. Recombinational repair of DNA damage in Escherichia coli and bacteriophage lambda. Microbiol Mol Biol Rev. 1999; 63:751–813. [PubMed: 10585965]
20. Ennis DG, Amundsen SK, Smith GR. Genetic functions promoting homologous recombination in Escherichia coli: a study of inversions in phage lambda. Genetics. 1987; 115:11–24. [PubMed: 2951295]
21. Glassberg J, Meyer RR, Kornberg A. Mutant single-strand binding protein of Escherichia coli: genetic and physiological characterization. J Bacteriol. 1979; 140:14–9. [PubMed: 227832]
22. Golub EI, Low KB. Indirect stimulation of genetic recombination. Proc Natl Acad Sci U S A. 1983; 80:1401–5. [PubMed: 6219392]
23. Umezu K, Chi NW, Kolodner RD. Biochemical interaction of the Escherichia coli RecF, RecO, and RecR proteins with RecA protein and single-stranded DNA binding protein. Proc Natl Acad Sci U S A. 1993; 90:3875–9. [PubMed: 8483906]
24. Anderson DG, Kowalczykowski SC. The translocating RecBCD enzyme stimulates recombination by directing RecA protein onto ssDNA in a chi-regulated manner. Cell. 1997; 90:77–86. [PubMed: 9230304]
25. Bork JM, Cox MM, Inman RB. The RecOR proteins modulate RecA protein function at 5' ends of single-stranded DNA. Embo J. 2001; 20:7313–22. [PubMed: 11743007]
26. Morimatsu K, Kowalczykowski SC. RecFOR proteins load RecA protein onto gapped DNA to accelerate DNA strand exchange: a universal step of recombinational repair. Mol Cell. 2003; 11:1337–47. [PubMed: 12769856]
27. Hobbs MD, Sakai A, Cox MM. SSB Protein Limits RecOR Binding onto Single-stranded DNA. J Biol Chem. 2007; 282:11058–67. [PubMed: 17272275]
28. Chen Z, Yang H, Pavletich NP. Mechanism of homologous recombination from the RecA-ssDNA/dsDNA structures. Nature. 2008; 453:489–494. [PubMed: 18497818]
29. Kowalczykowski SC, Clow J, Somani R, Varghese A. Effects of the Escherichia coli SSB protein on the binding of Escherichia coli RecA protein to single-stranded DNA. Demonstration of competitive binding and the lack of a specific protein-protein interaction. J Mol Biol. 1987; 193:81–95. [PubMed: 3295259]
30. Kowalczykowski SC, Krupp RA. Effects of Escherichia coli SSB protein on the single-stranded DNA-dependent ATPase activity of Escherichia coli RecA protein. Evidence that SSB protein

facilitates the binding of RecA protein to regions of secondary structure within single-stranded DNA. J Mol Biol. 1987; 193:97–113. [PubMed: 2953903]

31. Muniyappa K, Shaner SL, Tsang SS, Radding CM. Mechanism of the concerted action of recA protein and helix-destabilizing proteins in homologous recombination. Proc Natl Acad Sci U S A. 1984; 81:2757–61. [PubMed: 6326142]
32. Eggington JM, Kozlov AG, Cox MM, Lohman TM. Polar destabilization of DNA duplexes with single-stranded overhangs by the Deinococcus radiodurans SSB protein. Biochemistry. 2006; 45:14490–502. [PubMed: 17128988]
33. Bujalowski W, Lohman TM. Limited co-operativity in protein-nucleic acid interactions. A thermodynamic model for the interactions of Escherichia coli single strand binding protein with single-stranded nucleic acids in the “beaded”, (SSB)65 mode. J Mol Biol. 1987; 195:897–907. [PubMed: 3309344]
34. Romer R, Schomburg U, Krauss G, Maass G. Escherichia-Coli Single-Stranded-DNA Binding-Protein Is Mobile on DNA - H-1-Nmr Study of Its Interaction with Oligonucleotide and Polynucleotide. Biochemistry. 1984; 23:6132–6137. [PubMed: 6395890]
35. Clendenning JB, Schurr JM. A model for the binding of E. coli single-strand binding protein to supercoiled DNA. Biophys Chem. 1994; 52:227–49. [PubMed: 7999974]
36. Glikin GC, Gargiulo G, Rena-Descalzi L, Worcel A. Escherichia coli single-strand binding protein stabilizes specific denatured sites in superhelical DNA. Nature. 1983; 303:770–4. [PubMed: 6306467]
37. Sun W, Godson GN. Structure of the Escherichia coli primase/single-strand DNA-binding protein/phage G4oric complex required for primer RNA synthesis. J Mol Biol. 1998; 276:689–703. [PubMed: 9500915]
38. Shereda RD, Bernstein DA, Keck JL. A Central Role for SSB in Escherichia coli RecQ DNA Helicase Function. J Biol Chem. 2007; 282:19247–58. [PubMed: 17483090]
39. Lecointe F, et al. Anticipating chromosomal replication fork arrest: SSB targets repair DNA helicases to active forks. Embo J. 2007
40. Richard DJ, et al. Single-stranded DNA-binding protein hSSB1 is critical for genomic stability. Nature. 2008
41. Rasnik I, McKinney SA, Ha T. Nonblinking and long-lasting single-molecule fluorescence imaging. Nat Methods. 2006; 3:891–3. [PubMed: 17013382]

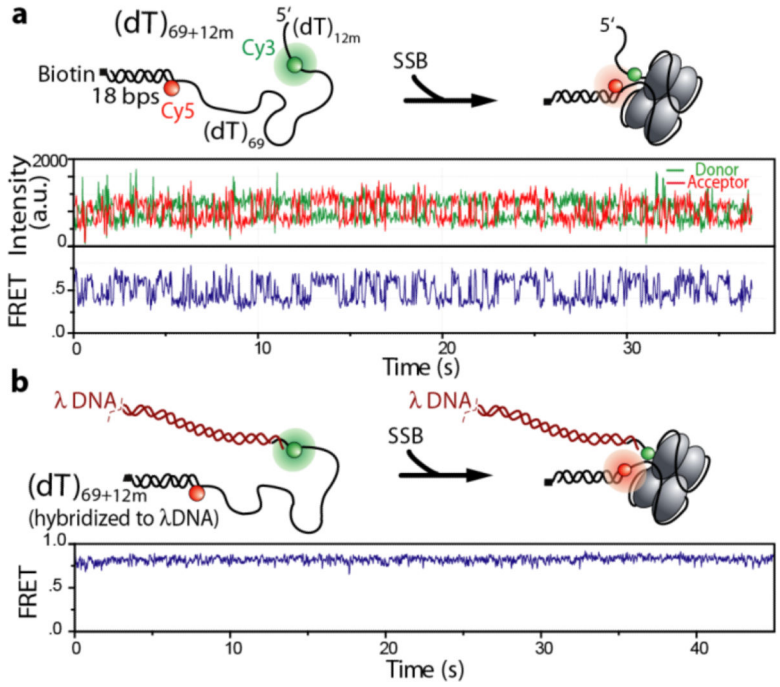

Figure 1. FRET fluctuations arising from diffusional migration of SSB on ssDNA

(a) With the 12 nt extension to the $(dT)_{69}$ separating the donor and acceptor fluorophores, rapid fluctuations between multiple FRET states are observed due to diffusion of SSB on the ssDNA. (b) When the 12 nt extension is hybridized to a complementary sequence, only steady high FRET values is observed.

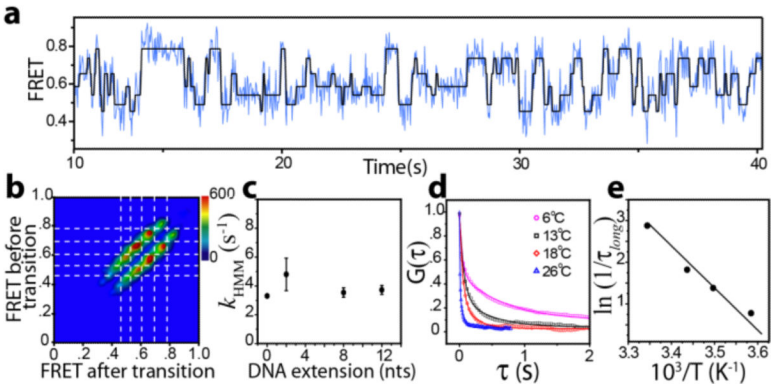

Figure 2. Analysis of SSB mobility on ssDNA

(a) Hidden Markov Model (HMM)-derived idealized FRET trajectory (black) superimposed on the FRET trajectory (blue) of a single SSB- $(dT)_{69+8}$ complex. (b) Transition density plot for $(dT)_{69+8}$ DNA. (c) Average rates of SSB migration as a function of DNA extension length from HMM analysis. Error bars are standard error over 2*(*m*-1) values of the transition rate obtained from HMM analysis where *m* is the number of distinct FRET states ranging from 2 to 6. (d) Autocorrelation (G(◇)) analysis of FRET trajectories for $(dT)_{69+8}$ DNA fit to bi-exponential decay function for different temperatures (T). (e) Arrhenius plot of apparent rates as a function of 1/T.

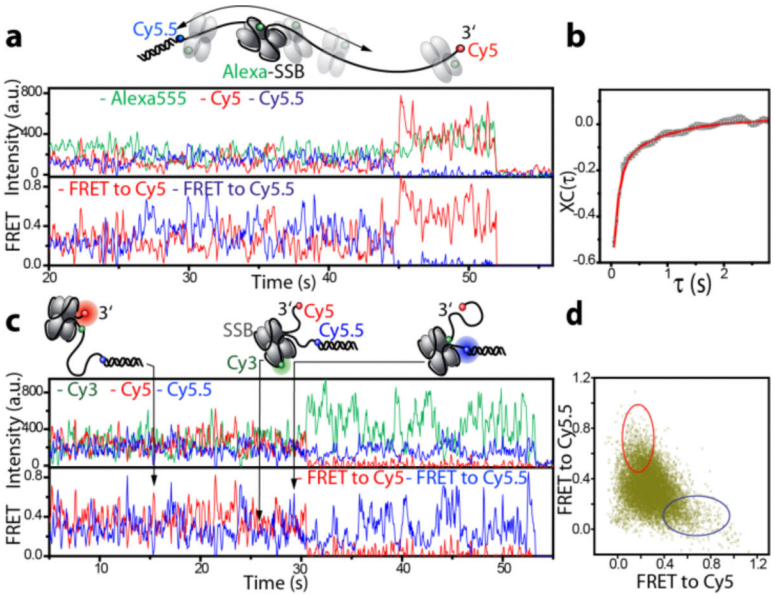

Figure 3. SSB diffusion on ssDNA probed with three-color FRET

(a) Time traces of three color intensities and the FRET efficiencies ($E_{app,5}$, $E_{app,5.5}$) display diffusion of donor-labelled SSB to acceptor labelled ends of a $(dT)_{130}$ DNA. (b) The average cross-correlation XC(τ) between $E_{app,5}$ and $E_{app,5.5}$ time traces (48 molecules) fit with a bi-exponential decay (red), demonstrates anti-correlated fluctuations. (c) A $(dT)_{130}$ with a centrally placed donor, and acceptors at the two ends, displays excursions of unlabelled SSB to either extremity of the DNA resulting in high FRET for the corresponding acceptor. (d) Scatter plot of $E_{app,5.5}$ vs. $E_{app,5}$ values (35 molecules) show mutually exclusive high FRET events (oval regions).

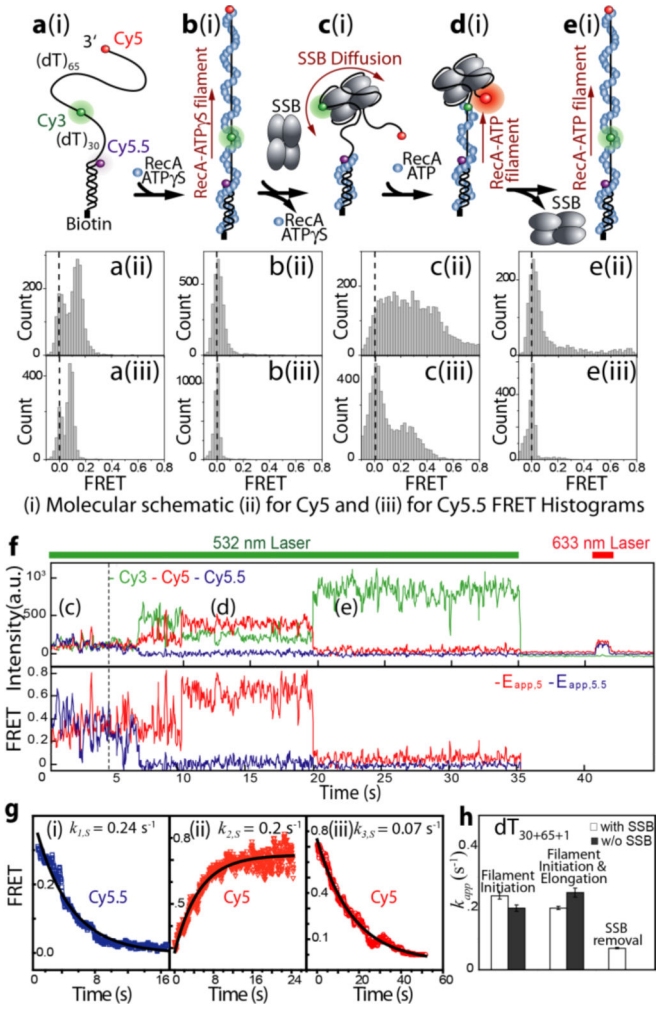

Figure 4. Mechanism of SSB displacement by an extending RecA filament

(a-e) (i) Schematic of reaction steps. (ii) $E_{app,5}$ histograms. (iii) $E_{app,5.5}$ histograms. (a) DNA construct with Cy3, Cy5 and Cy5.5. (b) RecA-ATPγS filament (5 min incubation). (c) SSB displaces RecA filament (15 min incubation). (d) RecA filament growth. (e) Filament completion (2 min incubation). (f) 3-color FRET trajectories for segments (c), (d) and (e). 633 nm excitation at 41 sec confirms active acceptors. (g) Sub-reaction kinetics with exponential fits (n= 46 molecules). (i) Average $E_{app,5.5}$ decay. (ii) Average $E_{app,5}$ increase. (iii) Average $E_{app,5}$ decay after maximum. (h) The rates of RecA filament initiation and elongation, and of SSB removal. Error bars are propagated standard errors from exponential fits in (g)

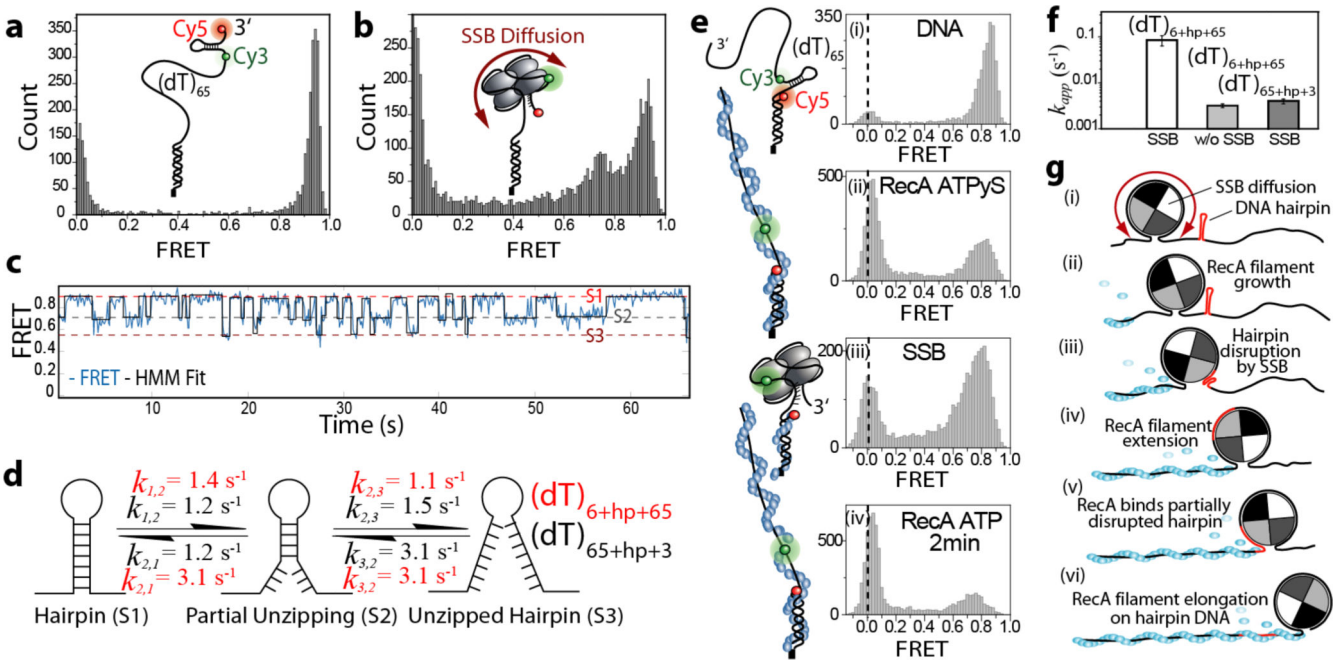

Figure 5. SSB diffusion promotes RecA filament growth on DNA hairpin

(a) FRET histograms for $(dT)_{65+hp+3}$. (b) Hairpin destabilization by SSB induces lower FRET states. (c) FRET trajectory of $(dT)_{65+hp+3}$ shows fluctuations between states S1 (intact hairpin), and S2 and S3 (unzipped hairpin states); HMM-derived idealized trajectory (black). (d) Transition rates between S1, S2 and S3 for $(dT)_{65+hp+3}$ and $(dT)_{6+hp+65}$. (e) SSB-assisted RecA filament formation on hairpin DNA. (i) Intact hairpin. (ii) RecA-ATPγS filament formation on a majority of DNA. (iii) SSB replaces the RecA-ATPγS filament restoring high FRET. (iv) RecA and ATP removes the hairpin structure. (f) The rates of hairpin removal by extending RecA-ATP filament vs. hairpin position. Error bars are standard errors based on two independent experiments each. (g) Model of SSB-assisted RecA filament growth on hairpin DNA.